Natural Hazards (2006) 38: 79–100
DOI 10.1007/s11069-005-8603-7

A Probabilistic Modelling System for Assessing Flood Risks

HEIKO APEL[1,★], ANNEGRET H. THIEKEN[1], BRUNO MERZ[1] and GÜNTER BLÖSCHL[2]
[1]*Section Engineering Hydrology, GeoForschungsZentrum Potsdam, Telegrafenberg, D-14473, Potsdam, Germany;* [2]*Institute of Hydraulics, Hydrology and Water Resources Management, Vienna University of Technology, Austria*

(Received: 2 June 2003; accepted: 1 September 2003)

Abstract. In order to be economically viable, flood disaster mitigation should be based on a comprehensive assessment of the flood risk. This requires the estimation of the flood hazard (i.e. runoff and associated probability) and the consequences of flooding (i.e. property damage, damage to persons, etc.). Within the "German Research Network Natural Disasters" project, the working group on "Flood Risk Analysis" investigated the complete flood disaster chain from the triggering event down to its various consequences. The working group developed complex, spatially distributed models representing the relevant meteorological, hydrological, hydraulic, geo-technical, and socio-economic processes. In order to assess flood risk these complex deterministic models were complemented by a simple probabilistic model. The latter model consists of modules each representing one process of the flood disaster chain. Each module is a simple parameterisation of the corresponding more complex model. This ensures that the two approaches (simple probabilistic and complex deterministic) are compatible at all steps of the flood disaster chain. The simple stochastic approach allows a large number of simulation runs in a Monte Carlo framework thus providing the basis for a probabilistic risk assessment. Using the proposed model, the flood risk including an estimation of the flood damage was quantified for an example area at the river Rhine. Additionally, the important influence of upstream levee breaches on the flood risk at the lower reaches was assessed. The proposed model concept is useful for the integrated assessment of flood risks in flood prone areas, for cost-benefit assessment and risk-based design of flood protection measures and as a decision support tool for flood management.

Key words: flood risk, probabilistic model, flood damage estimation, levee failure

ABBREVIATIONS: a.s.l. – above sea level; AMS – annual maximum series; BL – levee breach location; CDF – cumulated probability density function; CPU – central processor unit; LC – levee crest; LF – levee foot; MC – Monte Carlo; QD – direct discharge; QD_{max} – maximum direct discharge; QD_{norm} – normalised direct discharge; Q_{LC} – discharge at levee crest; t_{norm} – normalised time; t_{Qdmax} – time of maximum direct discharge; V_{pol} – volume of polder

★ Author for correspondence: Phone: +49-331-288 1514; Fax: +49-331-288 1570; E-mail: hapel@gfz-potsdam.de

1. Introduction

Flood defence systems are usually designed by specifying an exceedance probability and by demonstrating that the flood defence system prevents damage for events corresponding to this exceedance probability. This concept is limited by a number of assumptions and many researchers have called for more comprehensive design procedures (Plate, 1992; Bowles *et al.*, 1996; Berga, 1998; Vrijling, 2001). The most complete approach is the risk-based design which strives to balance benefits and costs of the design in an explicit manner (Stewart and Melchers, 1997). For example, an optimal flood defence system, chosen from multiple options, can be found by minimising the life-cycle costs, i.e. the expected costs during the lifetime of the system. The costs also include failure costs which relate to the adverse effects of system failure (monetary damage, loss of life, injury, etc.). Failure is defined as a state where the system does not fulfil its purpose, i.e. it does not provide safety. For example, failure of a river levee occurs when the levee's hinterland is inundated, e.g. because the river water level exceeds the levee crest or because the levee breaches due to internal erosion. In the context of risk-based design, flood risk encompasses the flood hazard (i.e. extreme events and associated probability) and the consequences of flooding (i.e. property damages). Ideally, a flood risk analysis should take into account all relevant flooding scenarios, their associated probabilities as well as their possible consequences and damages. Thus, a flood risk analysis should finally yield the full distribution function of the flood damages in the area under consideration.

In the past, comprehensive flood risk analyses have been an exception. Most analyses have been limited, e.g. by only considering a few failure scenarios or by neglecting the consequences of a failure. Such limitations in the analyses have often been the result of a lack of data or lack of knowledge of the complex interactions in predicting extreme events and their consequences. With advances in data acquisition and widespread availability of high-speed computerised tools, comprehensive flood risk analyses are becoming feasible and are gaining increased attention. This is a development that certainly can be observed in the field of dam safety (Berga, 1998).

The purpose of this paper is to present the methods and results of a comprehensive flood risk analysis developed within the framework of the German Research Network Natural Disasters (DFNK). The working group "Flood Risk Analysis" of the DFNK investigated the complete flood disaster chain from the triggering event to its consequences: "hydrological load – flood routing – potential failure of flood protection structures – inundation – property damage". The working group consisted of eight sub-projects which studied in detail the different processes of the flood disaster chain. For each element, complex, spatially distributed

models were applied, representing the meteorological, hydrological, hydraulic, geo-technical, and socio-economic processes (Grothmann and Reusswig, 2006; Holz *et al.*, 2006; Kamrath *et al.*, 2006; Menzel *et al.*, 2006). The standard way to quantify the flood risk is the combination of all processes of the flood disaster chain in a Monte-Carlo framework, which, however, involves an immense amount of CPU-time and difficulties with parameter estimation. This paper illustrates how the complex models can be complemented by a simple stochastic model consisting of modules each representing one process of the flood disaster chain. Each module is a simple parameterisation of the corresponding more complex deterministic model, where the parameterisations and parameters are calibrated against the data and results of the corresponding complex models. This ensures that the two approaches (simple probabilistic and complex deterministic) are compatible at all steps of the process chain.

Figure 1 shows an illustration of the two alternative strands representing the flood disaster chain. In the complex strand (left), the runoff processes are represented by stochastic rainfall simulations and spatially distributed catchment models; in the simple strand (right) the same processes are represented by the flood frequency curves and correlations between catchments. In the complex strand (left), the levee failure is represented by a geo-technical model; in the simple strand (right) the same processes are represented by the failure probabilities as a function of overtopping height and duration. In the complex strand (left), the damages are calculated by combining hydrodynamic simulations with a spatially distributed inventory of the property values; in the simple strand (right) damages are calculated from a damage function.

The advantages of the simple approach are numerous. First, significantly less CPU time is needed which allows application of the approach in Monte Carlo simulations. Second, the simple approach involves fewer parameters, so parameter estimation is more straightforward and robust. Third, the simpler model structure makes it easier for the analyst to understand the main controls of the systems. These advantages come at the expense of omitting some of the subtleties of the flood disaster chain.

In this paper, the feasibility of the simple approach is illustrated for a reach of the river Rhine in Germany. The flood risk, i.e. the distribution function of the direct monetary flood damage, is derived for a polder that is only inundated if the protecting levee system fails.

2. Investigation Area

As a target area, the reach of the Rhine between Cologne and Rees was selected with a focus on the polder at Mehrum (Figure 2). The polder at

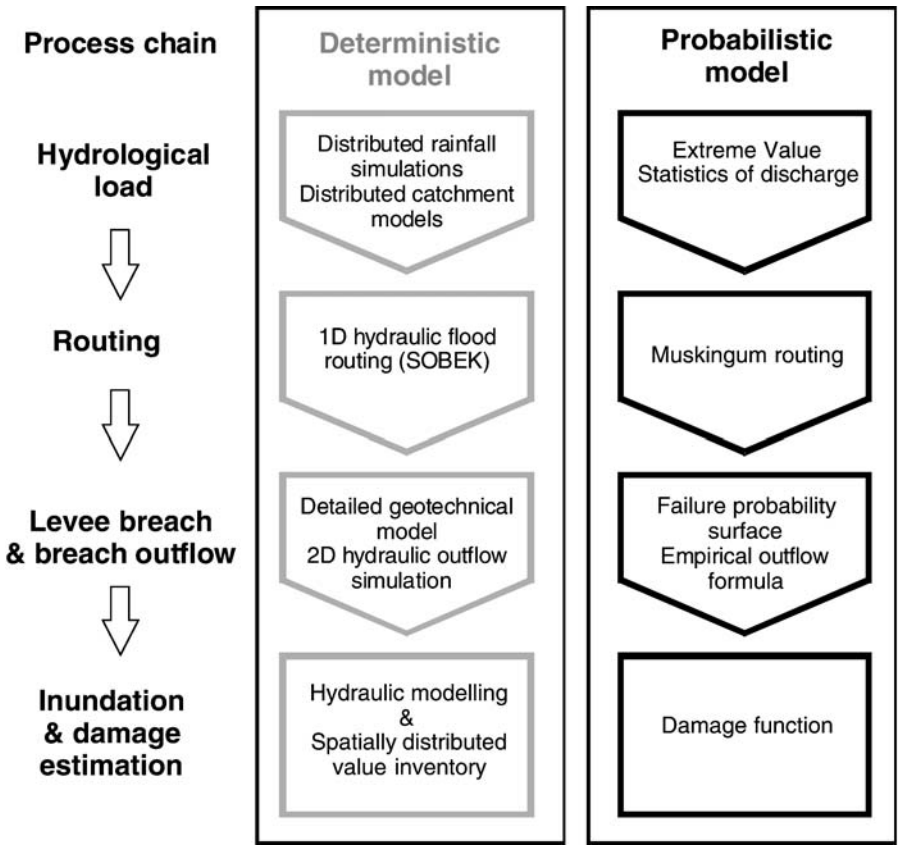

Figure 1. Scheme of the model components.

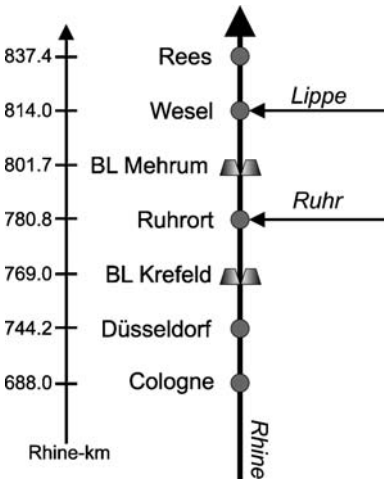

Figure 2. Schematic location of discharge gauges, levee breach locations (BL) and considered tributaries.

Table I. Basic geometric properties of levees at breach locations and polder volumes.

	levee foot (LF) [m a.s.l.]	levee crest (LC) [m a.s.l.]	discharge at LC Q_{LC}[m^3/s]	Volume of Polder at LC V_{pol} [m^3]
Krefeld	28.57	31.78	13,830	practically infinite
Mehrum	21.94	26.38	15,660	$6.43*10^7$ (at LC)

Mehrum is a rural area of 12.5 km^2, which is only inundated if the protecting levee system fails.

The model considers the following elements of the flood disaster chain: hydrological load, flood routing between the gauges Cologne and Rees, levee performance at two locations (Krefeld, Mehrum) and damage in the flooded areas within the polder at Mehrum (Figure 1). The two levee breach locations selected for the simulation differ significantly in their storing capacity. At Krefeld the large unbounded hinterland provides a retention basin with a practically infinite retention capacity whereas the polder at Mehrum is strictly confined to a comparatively small volume. The levees at the two breach locations are similar, but the levee crest is higher at Mehrum, i.e. larger flood waves are required to overtop the levee at Mehrum in comparison to Krefeld. Table I summarises the basic geometric properties of the levees along with the polder volumes.

3. Model and Input Data

The risk analysis for the flood disaster chain is based on the following modules:

- Hydrological load
- Flood routing
- Levee failure and outflow through levee breach
- Damage estimation
- Monte Carlo framework

3.1. HYDROLOGICAL LOAD

The hydrological load was derived from the flood frequency curve of the gauge Cologne/Rhine based on the annual maximum series from 1961 to 1995 (AMS 1961–1995). Four distribution functions were fitted to AMS 1961–1995: Gumbel, Pearson-III, Weibull and the Lognormal distribution. The four distribution functions were weighted by a Maximum Likelihood method to construct a composite probability distribution function (Wood and Rodriguez-Iturbe, 1975):

$$\bar{f}(q) = \sum_i \theta_i * f_i(q) \tag{1}$$

where $\bar{f}$: composite probability density function; f_i: individual pdfs; θ_i: Maximum Likelihood weights of the pdfs; q: annual maximum series; and

$$\theta_i = \frac{\prod_j f_i(q_j)}{\sum_i \left[\prod_j f_i(q_j) \right]} \tag{2}$$

with $i = 1, ..., 4$ denoting the distributions and $j = 1, ..., n$ the values of the annual maximum series.

This method gave the following weights θ_i for the individual distributions and AMS 1961–1995: Gumbel: $\theta_1 = 0.0743$; Lognormal: $\theta_2 = 0.1525$; Weibull: $\theta_3 = 0.3270$; Pearson III: $\theta_4 = 0.4463$

Figure 3 shows the four individual distributions and the composite distribution as well as their agreement with the empirical exceedance probabilities of the observed data (AMS 1961–1995) which were estimated by

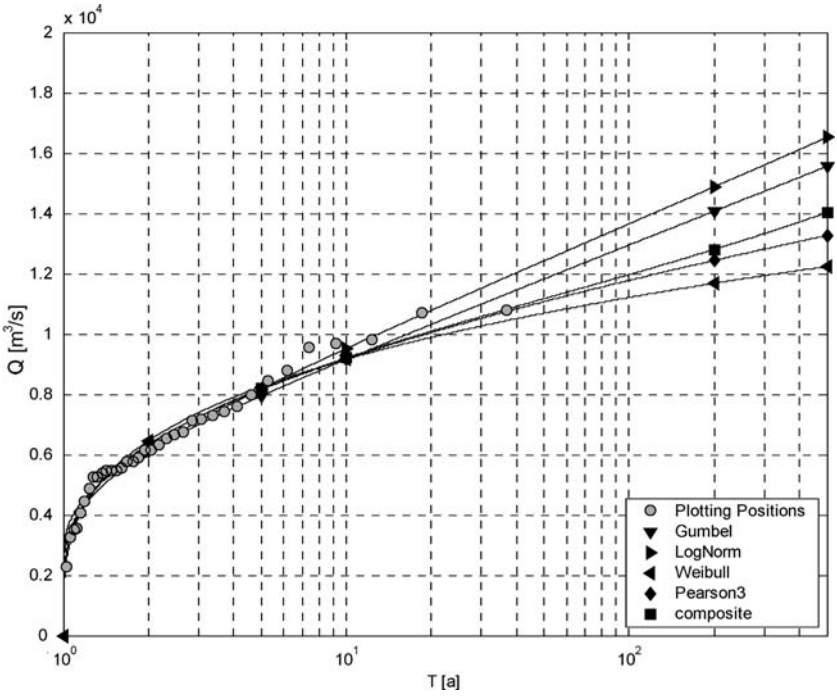

Figure 3. Different distribution functions fitted to the annual maximum flood series 1961–1995 of the gauge Cologne/Rhine.

Weibull plotting positions. The composite distribution function is most similar to the Pearson III distribution.

In order to determine levee breaches and inundation levels of the polders it was necessary to generate flood hydrographs in addition to the maximum discharge. Hence typical flood hydrographs were generated at the gauge Cologne by means of non-dimensional or normalised hydrographs (Dyck and Peschke, 1995) in combination with cluster analysis.

For each flood event of the series AMS 1961–1995 a normalised hydrograph of the direct runoff was calculated as follows (Dyck and Peschke, 1995):

- Baseflow QB was separated from total runoff Q assuming a linear baseflow hydrograph between the beginning and the end of direct runoff.
- The direct peak flow QD_{max} and the time to peak t_{QDmax}were determined.
- The hydrograph of the direct runoff QD was normalised by

$$QD_{norm} = QD/QD_{max} \quad \text{(direct runoff)} \tag{3}$$

$$t_{norm} = t/t_{QD_{max}} \quad \text{(time)} \tag{4}$$

so that the scaled direct peak flow is unity at time 1.

The normalised hydrographs of direct runoff within the AMS 1961–1995 were finally scaled to a consistent duration of $t_{norm} = 10$.

In order to find typical shapes of the hydrographs, cluster analysis with Euclidian distance and the *average-linkage-between-groups-algorithm* was applied twice. All normalised hydrographs were included in the first cluster analysis, which yielded the dendrogram shown in Figure 4a. A split of five clusters gives four small clusters containing one to three events and one big

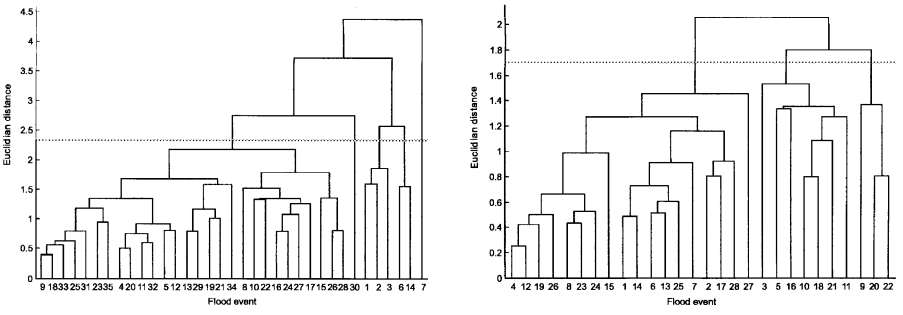

Figure 4. Dendrogram of the cluster analyses (Euclidian distance, average linkage between groups) of normalised hydrographs. (a) all 35 normalised hydrographs (normalised time: $0 \leq t_{norm} \leq 10$), (b) 28 hydrographs (big cluster of analysis A, normalised time: $0 \leq t_{norm} \leq 2$).

Table II. Mean parameters (peak flow, time to peak, baseflow) for each cluster at stream gauge Cologne (Rhine).

	Counts	Peak flow [m^3/s]	Time to peak [d]	Flood duration [d]	Initial baseflow [m^3/s]	Final baseflow [m^3/s]
Analysis A						
Cluster 1	3	4,750	6.3	36.0	1,400	2,100
Cluster 2	2	5,730	13.5	43.5	1,535	2,150
Cluster 3	28	6,682	16.6	35.8	1,647	2,151
Cluster 4	1	7,600	8.0	35.0	1,270	1,990
Cluster 5	1	7,290	6.0	35.0	2,480	2,680
Analysis B						
Cluster 31	7	7,190	29.9	47.7	1,492	2,163
Cluster 32	3	7,063	21.3	41.3	1,997	2,590
Cluster 33	18	6421	10.7	30.3	1,650	2,072

Analysis A: all 35 normalised hydrographs (normalised time: $0 \leq t_{norm} \leq 10$), Analysis B: 28 hydrographs (cluster 3 of analysis A, normalised time: $0 \leq t_{norm} \leq 2$).

cluster of 28 events (Table II). The small clusters exhibit rather small times to peak of 6–13 days (cluster 1, 2, 4 and 5 in Table II) and the maximum peak flow is succeeded by multiple smaller peaks (cluster 1, 2, 4 and 5 in Figure 5). The big cluster, however, exhibits a considerably larger time to peak and the hydrograph is single peaked ending at a normalised time of $t_{norm} \approx 3$.

As a result of the normalisation of both the time and the flow axes to unity, the time period between the beginning of direct runoff and the peak ($0 \leq t_{norm} \leq 1$) is less represented in this cluster analysis than the time between the peak and the end of direct runoff ($1 < t_{norm} \leq 10$). Therefore, the big cluster (cluster 3 of the first analysis) was subjected to a second cluster analysis where the normalised hydrographs with $0 \leq t_{norm} \leq 2$ were considered. Here (Figure 4b), the three cluster solution was chosen. While cluster 33 still shows a uniform hydrograph with a single peak, the hydrographs of cluster 31 and cluster 32 have multiple peaks preceding the maximum peak flow. Also, their time to peak is considerably longer (Table II). The result of this procedure are seven different types of typical, realistic hydrographs: single peaked hydrographs and various multiple peaked hydrographs (Figure 5). Within the Monte Carlo framework (see section 3.5) the normalised hydrographs were rescaled using the flood frequency statistics at Cologne and the parameters in Table II.

Since the major tributaries in the selected reach Lippe and Ruhr were also considered in the model, their maximum discharges and the shape of their hydrographs had to be determined, too. The peak discharges in the main river (gauge Cologne, Rhine) and the discharges of the corresponding

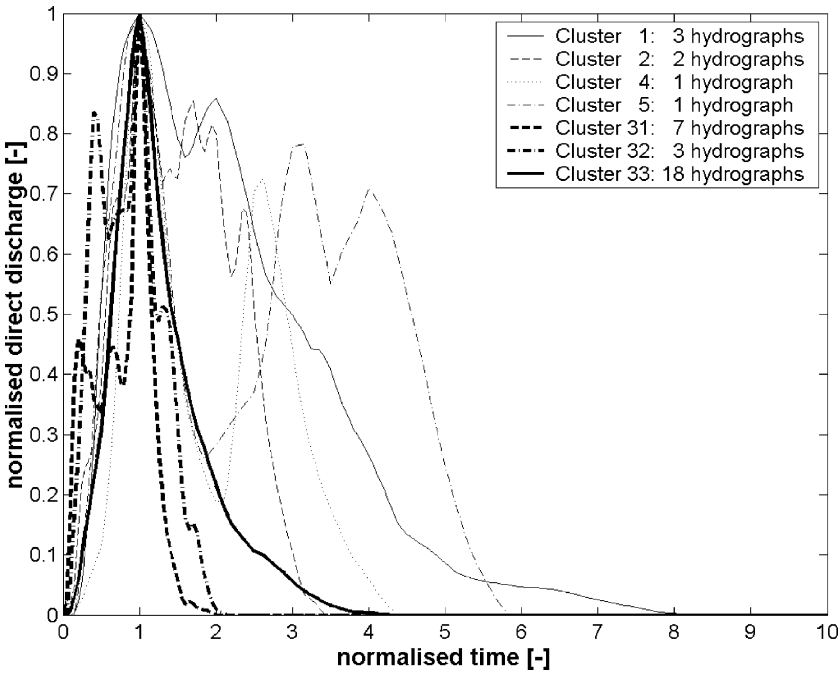

Figure 5. Normalised and clustered hydrographs of direct runoff from 35 annual maximum events at gauge Cologne (Rhine) (AMS 1961–1995).

Table III. Correlation between the peak flows in annual maximum series AMS 1961–1995 (Cologne, Rhine) and the peak discharges of the corresponding events in the tributaries.

	Cologne, Rhine	Hattingen, Ruhr
Hattingen, Ruhr	0.60	
Schermbeck I, Lippe	0.62	0.91

events in the tributaries (gauge Schermbeck I (Lippe) and gauge Hattingen (Ruhr)) in the AMS 1961–1995 are correlated (Table III) and their relationship is approximately linear (Figure 6). Therefore, peak discharges at the tributaries were generated based on linear regressions and the correlations between main river and tributaries (cf. 3.5). The mean shapes of the hydrographs in the tributaries were determined for each cluster in Table II, i.e. the hydrographs of the tributaries corresponding to those at the main river were identified.

3.2. FLOOD ROUTING

The second module of the flood disaster chain is a routing module consisting of the Muskingum routing method for flood waves in river channels

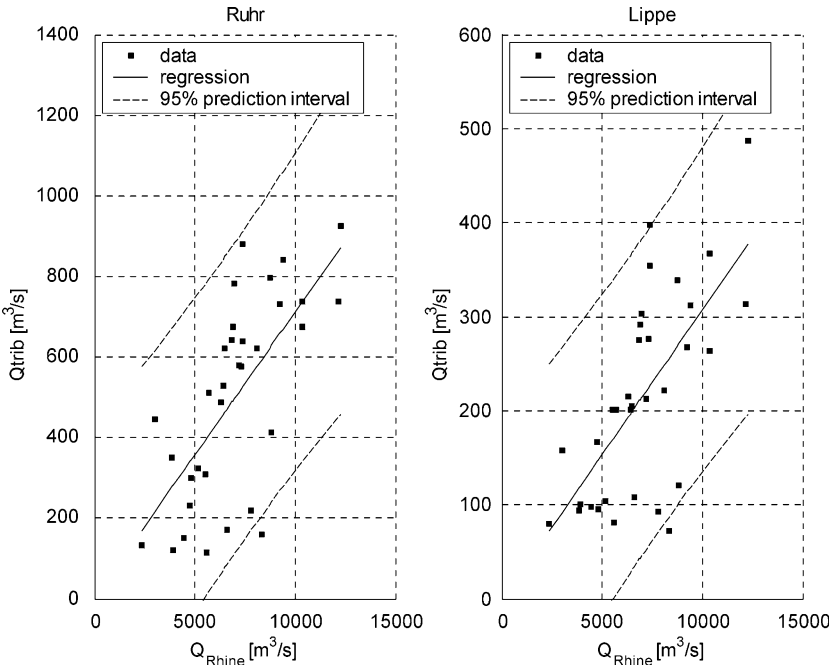

Figure 6. Linear regressions between maximum discharge of the Rhine (gauge Cologne) and maximum discharge of the tributary rivers Ruhr (gauge Hattingen) and Lippe (gauge Schermbeck I) of the corresponding events with 95% prediction intervals for annual maximum series AMS 1961–1995 of the Rhine at Cologne.

(Maidment, 1992). The required parameters, travel time K and form parameter m, were estimated for the defined river reaches from the 35 flood events of the years 1961–1995, which were simulated with the 1-dimensional, non-stationary hydrodynamic model SOBEK (Kamrath *et al*., 2006). The travel times for the reaches were calculated as the mean travel times K of the peak discharges between the gauging stations, whereas the form parameter m was estimated from the complete flood waves utilising a Minimisation of Least Squares method.

3.3. LEVEE FAILURE AND OUTFLOW THROUGH LEVEE BREACH

For the calculation of the failure probability of a levee, a general engineering technique was applied in which a breach condition is defined as the exceedance of a load factor over a resistance factor. Applying this concept to the most important failure mechanism for new river levees, the breaching due to overtopping, the breach criterion is defined as the difference q_D between the actual overflow q_a [m^3/s] (the load factor) and the critical overflow q_{crit} [m^3/s] (the resistance factor):

$$\text{if} \quad q_{\text{a}} > q_{\text{crit}} \rightarrow \text{breach} \tag{5}$$

or

$$\text{if} \quad q_{\text{D}} > 0 \rightarrow \text{breach}$$

where

$$q_{\text{D}} = q_{\text{a}} - q_{\text{crit}}$$

$$q_a = \text{A} \cdot dh^{3/2} \quad \text{(Kortenhaus and Oumeraci, 2002)} \tag{6}$$

$$q_{\text{crit}} = \frac{v_c^{5/2} \cdot k^{1/4}}{125 \tan \alpha_i^{3/4}} \quad \text{(Vrijling, 2000)} \tag{7}$$

$$v_c = f_g \frac{3.8}{1 + 0.8 \log_{10}(t_e)} \tag{8}$$

and where $A[\text{m}^2/\text{s}]$ is a summary parameter representing the geometric features of the levee (see Kortenhaus and Oumeraci, 2002 for details), dh[m] is the difference between the water level and the levee crest, ν_c [m/s] is the critical flow velocity, α_i [deg] the angle of the inner talus, k[m] the roughness of the inner talus, f_g [ ] a parameter describing the quality of the levee turf and t_e the overflow duration [h].

Based on this intermediate complex deterministic model a probabilistic model describing the conditional failure probability depending on overtopping height and time is derived. In order to calculate the failure probability, the method of derivation of *conditional levee failure curves* described in USACE (1999) was extended in this work. Since the definition of the failure criterion in (5) contains two independent variables, dh and t_e, it was necessary to construct a conditional failure probability surface instead of a one-dimensional failure curve. The derivation of the conditional failure surface for each breach location comprises the following steps:

- Description of the uncertainty of the parameters in (6)–(8), i.e. estimates of mean values, standard deviations or coefficients of variance and distribution types. Values or estimates of these moments can be found in Vrijling (2000).
- Perform a Monte Carlo (MC) simulation using a fixed pair of (dh, t_e) to calculate the breach criterion $q_{\text{a}} - q_{\text{crit}}$. In this step, 10^4 MC-samples per pair of independent variables were simulated.
- Calculate the moments of the MC-simulation results and identify an appropriate distribution type.

– Extract the probability of exceedance of the breach criterion $q_a - q_{crit} = 0$ from the cumulative distribution of the MC-simulation result. This is the failure probability of the levee for a given overflow height *dh* after a given duration t_e.
– Repeat the procedure for other pairs of (dh t_e)
– Construct the failure surface from the failure probabilities of the (dh, t_e)-tuples.

As an example, Figure 7 shows the results of a single MC-simulation for $dh = 0.15$ m and $t_e = 3$ h. Figure 8 shows the resulting failure probability surface for the breach location Krefeld.

The outflow through a levee breach is calculated from an empirical outflow formula presented in Kamrath *et al*. (2006). This formula is based on the standard weir formula of Poleni, but with enhanced empirical relationships between the weir coefficient and geometric and hydromechanic parameters of the levee and the river. These relationships were calibrated for the Lower Rhine at the selected breach locations, using the 2-dimensional breach outflow simulations performed by Holz *et al*. (2006). From this formula it

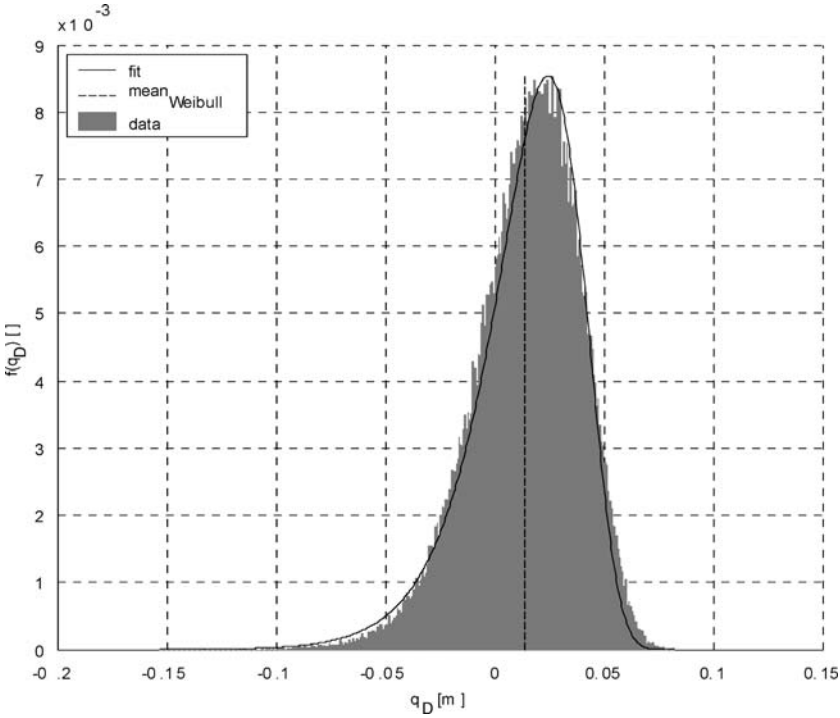

Figure 7. Fit of the Weibull-distribution to MC-simulation result for $dh = 0.15$ m and $t_e = 3$ h; MC sample size $= 10^4$, goodness of fit: $R^2 = 0.99956$ (fit to CDF).

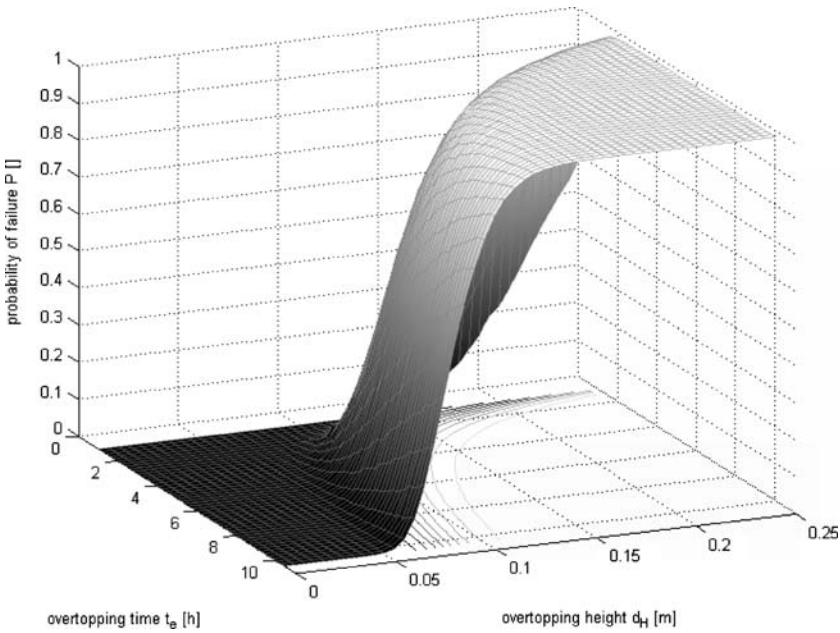

Figure 8. Levee failure probability surface for breach location Krefeld derived with the proposed procedure.

was possible to calculate the outflow through a levee breach depending upon the water levels of river and polder and the breach dimensions.

However, for the temporal and spatial breach development at the two breach locations no functional relationship could be found due to the very complex breach mechanism and the high variability in the factors influencing the breach development (Singh, 1996). Therefore, some simplifying assumptions were made based on an expert assessment. It was assumed that the breach development is completed within 1 h. This is a reasonable and justifiable assumption since the temporal development of a breach is quick within minutes to a couple of hours and has consequently little impact on the overall expected damage in the hinterland. The spatial development, however, is more important and more uncertain. Knowledge about levee breach widths is very limited and mostly based on empirical evidence only. In this paper, therefore, the risk assessment was performed for a number of scenarios of different breach widths at Krefeld, varying the widths from 100 to 400 m, and a fixed width of 100 m at Mehrum. The choice of a fixed breach width at Mehrum is justifiable by the small volume of the polder, which is filled within a very short time even in case of a small breach width of, say, 100 m. This means that the flood retention capacity of the polder at Mehrum is determined by the volume of the polder rather than by the dimension of the levee breach, as it is the case at

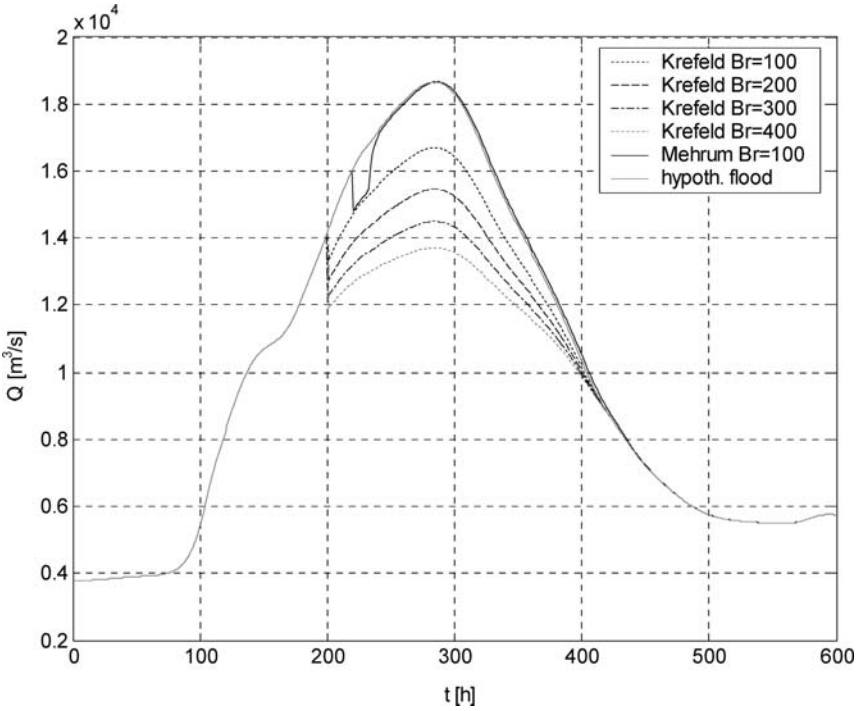

Figure 9. Reduction of a hypothetical flood by levee breaches at Krefeld and Mehrum. The hypothetical flood is the flood of 1995 scaled by a factor of 1.5; Br = breach width in *m*.

Krefeld. Figure 9 shows the reduction of a hypothetical flood for breaches at Krefeld and Mehrum, where the same flood wave was used for the two breach locations, i.e. the travel time and reshaping of the flood wave from Krefeld to Mehrum was neglected in this case. It can be seen from Figure 9 that the very large storage capacity of the polder at Krefeld significantly decreases the flood wave, whereas the outflow into the polder at Mehrum has only a marginal effect on the peak discharge.

3.4. DAMAGE ESTIMATION IN INUNDATED AREAS

The last module estimates direct monetary losses within the polder at Mehrum. Flood damage can only occur if the levee system at Mehrum fails. Since inundated areas were not calculated directly by the model, a damage function that relates the damage in inundated areas in the polder at Mehrum to the inflow water volume after/during a levee failure had to be determined. This was done by assuming the filling of the polder in 0.5 m steps up to the levee crest and intersecting each inundation layer with the land use map and the digital elevation model. The damage of the

Table IV. Economic damage per sector in the polder at Mehrum.

Economic sector	Area in the polder at Mehrum [m^2]	Replacement value 2000 [€/m^2]
Private housing	471,100	562.14
Manufacturing and building industry	4,300	244.87
Public infrastructure	30,500	466.51
Energy and water supply	19,700	1784.58
Traffic and communication engineering	400	41.07
Buildings in agriculture and forestry	511,000	48.46
Agricultural area, forest and others	11,653,900	–
Total	12,690,900	–

inundated land use types was estimated by combining assessed replacement values and stage-damage curves:

$$D_{\text{sec}} = \text{AIN}_{\text{sec}} \cdot d_{\text{sec}}(h) \cdot V_{\text{sec}} \tag{9}$$

where D_{sec} total direct property damage per economic sector [€], AIN_{sec} inundated area per economic sector [km^2], $d_{sec}(h)$ average property damage per economic sector as a function of the inundation depth [–], v_{sec} sector-specific economic value [€/m^2]

The sector-specific economic values are independent from a given inundation scenario. They were determined from the economic statistics of Northrhine–Westphalia from 1997 (capital stock data according to the system of national accounts from 1958 and land use information from the statistical regional authorities in Northrhine–Westphalia). The replacement values were scaled to the year 2000 by data on the development of capital stocks in Northrhine–Westphalia (1995: 100; 1997: 102.8; 2000: 108.2) and adjusted to Mehrum by comparing the gross value added per employee in that region with that of entire Northrhine-Westphalia. Values in the sector of private housing were assessed by the number of buildings, households and cars in the target area and their respective average insured capital in 2000. Appropriate data were provided by the German Insurance Association. All replacement values for Mehrum are summarized in Table IV.

The distribution of the economic sectors (industry, private housing, infrastructure etc.) within the polder at Mehrum was given by a land register – the German official topographic–cartographic information system ATKIS (Table IV). This analysis yields a total value of 340 Mio. € for the assets (buildings and contents) in the polder at Mehrum.

The average property damages per economic sector $d_{sec}(h)$ depend on the inundation depth. Stage-damage functions were derived in accordance

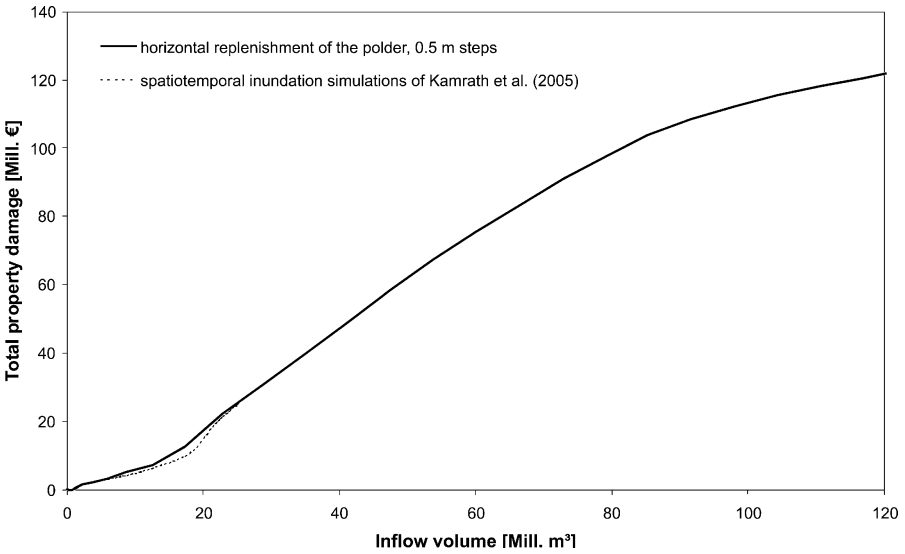

Figure 10. Direct property damage within the polder at Mehrum as a function of the inflow volume after/during a levee failure.

with ProAqua (2000, unpublished). Damage was determined per inundated grid cell using Equation (9). The total damage of a scenario amounts to the sum of the damages of all grid cells. The resulting relationship between inflow volume and property damage in the polder at Mehrum based on a step-by-step replenishment of the polder is shown in Figure 10. With the used stage-damage curves a maximum damage of 120 Mill. € may occur which amounts to 35% of the estimated values.

The curves so estimated were compared to damage estimates based on space-time patterns of inundation after a levee failure at Mehrum simulated by Kamrath *et al.* (2006). Figure 10 shows that our results are very similar to those of the more detailed analysis of Kamrath *et al.* (2006).

3.5. MONTE CARLO FRAMEWORK

All modules were combined in a first order Monte Carlo framework. First, a discharge value was randomly chosen from the composite flood frequency curve at Cologne. Next, the flood type was randomly chosen according to the likelihood of the flood types identified by the cluster analysis. From discharge and flood type, a flood wave was constructed and then routed to the final gauge at Rees, with tests for levee breaches at Krefeld and Mehrum. The discharge was increased by discharges from the tributaries Ruhr and Lippe which were calculated on the basis of the main river – tributary regressions shown in Figure 6. In order to simulate the correlations between the main and tributary discharges, the tributary

discharge was randomised for any given main river discharge assuming a normal distribution with means calculated from the regression equations and standard deviations calculated from Equation (10):

$$\sigma_{\text{triB\_cor}} = \sigma_{\text{triB}}\sqrt{1-\rho_i^2} \quad \text{(Cullen and Frey, 1999)} \tag{10}$$

where ρ_i denotes the correlation coefficients (Table III). The randomised tributary discharges were additionally corrected to the base flow in case of randomised discharges smaller than the base flow. Using this procedure it was possible to represent both the functional relationships between main and tributary discharges as expressed in the regression formulae and the variability in the relationship as expressed in the correlation coefficients.

For the target area (polder at Mehrum) the discharges were, in a next step, transformed into direct property damages with the damage curve (Figure 10) to assess the flood risk. By repeating this procedure 10^5 times, the distribution function of input discharge at Cologne was transformed into a distribution function of property damage at the Polder Mehrum. This distribution was plotted as a risk curve which represents the return interval of events associated with a damage exceeding a given level.

To account for the uncertainties of the spatial breach development (Section 3.3), the procedure described above was performed for five different scenarios K0, K100, K200, K300 and K400 with breach widths of 0–400 m at Krefeld. For all scenarios, the same set of randomised maximum discharges for the main river Rhine was used in order to accurately assess the influence of breach widths at Krefeld on the failure probabilities at Mehrum.

4. Results

The results of the MC-simulations for the five scenarios show a significant effect of the upstream levee breaches on the risk of levee breaches and flood damages downstream (Table V). Without any upstream breaches, the levee at Mehrum failed 92 times (failure rate 0.92‰) in the MC-simulations.

Table V. Number of levee breaches in the 10^5 simulations for the five scenarios K0, K100, K200, K300 and K400 with breach widths of 0–400 m at Krefeld.

Scenario	Total no. of model runs with breaches	Krefeld	Mehrum
K0	92	–	92
K100	164	164	39
K200	162	162	20
K300	166	166	6
K400	161	161	1

When breaches at Krefeld were allowed, this figure was significantly reduced (to only one failure of the levee at Mehrum in the case of a breach width of 400 m at Krefeld, Table V). The flood frequency curve at Rees, the most downstream gauging station of the investigation area, is also influenced by the number of upstream levee breaches and the breach width at Krefeld. Figure 11 shows the frequency curves for the different scenarios derived from Weibull Plotting Positions of the output of the routing module. The return intervals associated with discharges larger than the critical discharge required for levee breaches differ as a function of the breach width. Overall, the exceedance probabilities of extreme events are reduced by upstream levee breaches while the exceedance probabilities of discharges at the critical levels are increased. This effect is caused by the reduction of a number of floods overtopping the levee to discharges below the critical overflowing discharge (Figure 9). The effect is more pronounced the wider the breach at Krefeld is assumed.

The risk curve for Mehrum was constructed from the calculated inflow volume of the polder for the different scenarios. Exemplarily Figure 12 shows the trajectories of the polder volume for the six breach events of scenario K300. It can be seen that the polder is quickly filled and levelled with the water level of the river. The expected damage for each breach

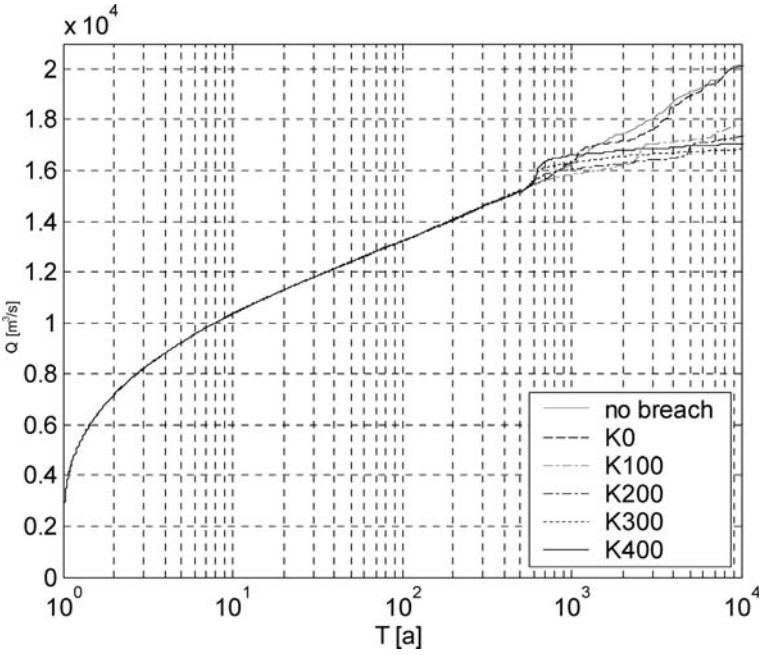

Figure 11. Frequency curves (interpolated Weibull Plotting Positions) at gauge Rees after routing and levee breaches for the five scenarios (Table V).

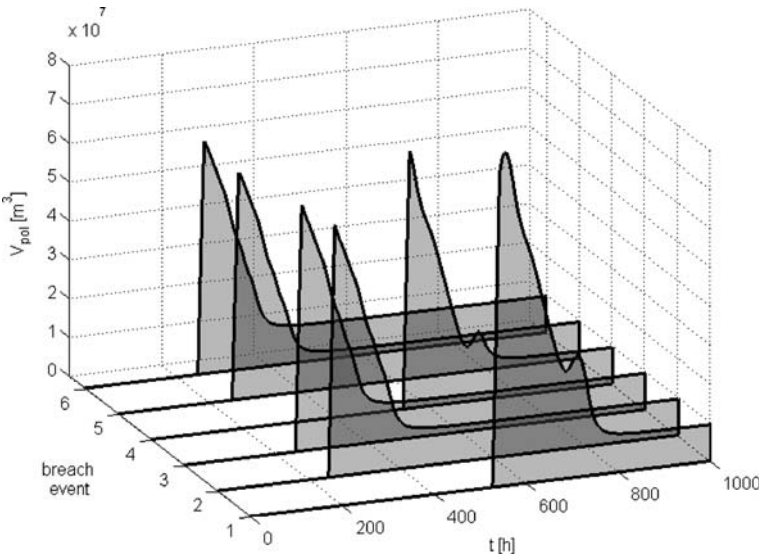

Figure 12. Filled volume of the polder at Mehrum during breach events of scenario K300.

event was calculated from the damage curve (Figure 10) and the maximum inflow volume of the breach events. By this procedure, the risk curve for the polder at Mehrum shown in Figure 13 was derived. The step-like trajectories of the risk curves are a result of the presence of the flood protection system as the damages only occur for discharges equal to or in excess of discharges causing levee failure. For breach widths at Krefeld larger than 300 m, the risk of damage at Mehrum is zero up to a return interval of 10^4 years which is a result of the high retention capacity of the upstream polder. This, again, emphasises the key role of upstream levee failures for the flood risk downstream.

5. Discussion and Conclusions

The proposed model quantifies the probability of levee failures caused by overtopping as well as the monetary damages in the target area. The stochastic approach allows a large number of simulation runs in a Monte Carlo framework in an acceptable time-frame. The flood risk analysis is therefore not restricted to a few scenarios but covers a wide variety of flood events. The randomised flood events not only differ in terms of peak discharges but also in terms of the shapes of the hydrographs and the tributary discharges. Therefore, the approach is amenable to integrated flood risk assessment.

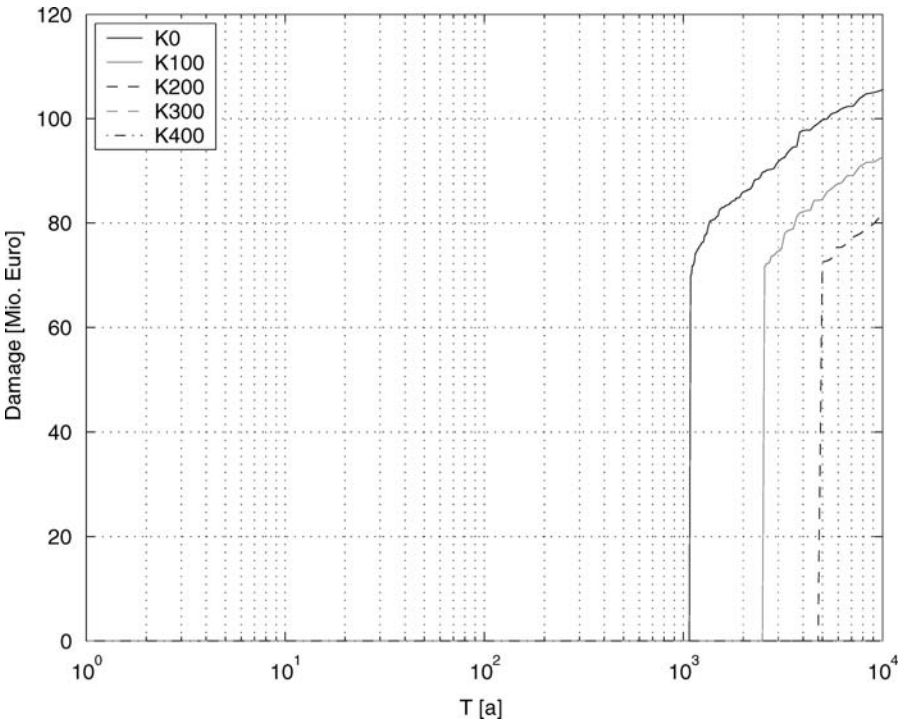

Figure 13. Flood risk curve for the polder at Mehrum. K0, K100, K200, K300 and K400 relate to breach widths of 0–400 m at Krefeld (damages in scenarios K300 and K400 have return intervals $>10^4$).

The results suggest that, in the area under investigation, upstream levee failures significantly affect the failure probability downstream and, hence the risk curve of the target area. The simulations also show the effect of the retention volume of a polder. Owing to the very large retention capacity of the hinterland at Krefeld the levee failure probability at Mehrum is significantly reduced and the flood frequency curve at Rees is attenuated if levee failures at Krefeld are allowed. The size of the polder at Mehrum in combination with the dimension of the flood protection structures control the shape of the flood risk curve. The step-like shape of the risk curve results from the small volume of the polder and the high magnitude of the events overtopping the levee. This means that once a levee fails due to overtopping, an immediate damage larger than 70 Mio. € has to be expected. But if breach widths of 300 m and larger are assumed for the breach location Krefeld, the risk for Mehrum is zero up to return intervals of 10^4 years. However this statement has to be treated with care, since the uncertainties involved in this risk assessment are not estimated to full extent at present. At the present state the flood frequency statistics (annual

maximum series) and the spatial breach development are considered in the uncertainty estimation. However, the model system allows the analysis of additional various sources of uncertainty like uncertainties associated to the stage-discharge relationship or the determination of levee breaches. In order to refine the uncertainty analysis, 2nd-order Monte-Carlo simulations will be performed in the future and confidence bounds on the risk curves will be constructed. However, since the estimated risks significantly depend on the width of upstream breaches, as shown by the scenario results, and since the likelihood of the breach width scenarios is unknown, an unknown portion of uncertainty will remain in this risk assessment. In order to address this problem, a study investigating the levee breaches during the August-2002 flood of the Elbe will be started soon.

Due to its modular structure and the universal nature of the methods used, the proposed model system should be transferable to other river systems provided the required data sets are available. In addition, single parts of the model system may be applied independently, e.g. to investigate the probability of levee failure at a given location. It is therefore believed that the system may be profitably used for a number of additional purposes, e.g. as a tool for cost-benefit analysis of flood protection measures, and as a decision support system for operational flood control. Another possible application is the flood management and control during a severe flood for which estimates of the effects of upstream levee breaches on the shape and propagation of the flood wave and thus on inundation risks at the reaches downstream may be useful. Real time simulations of such scenarios could facilitate the emergency management and enhance the efficiency of planned levee failures or weir openings. However, a prerequisite for these applications is an accurate calibration of the model system to a given reach. Clearly, this needs to be done prior to a severe flood event. This implies that, ideally, the flood risk estimation system should be applicable to both long-term planning tasks and operational decision support.

Acknowledgements

Funding from the German Ministry for Education and Research (project number 01SFR9969/5) and data provision from the Institute of Hydrology, Koblenz, Munich Re, Munich, the German Insurance Association (GDV), Berlin and ProAqua, Aachen are gratefully acknowledged.

References

Berga, L.: 1998. New trends in hydrological safety, in L. Berga (ed.), *Dam Safety* (pp. 1099–1106). Rotterdam: Balkema.

Bowles, D., Anderson, L., and Glover, T.: 1996, Risk assessment approach to dam safety criteria. Uncertainty in the Geologic Environment: From Theory to Practice. Geotechnical Special Publication No. 58, ASCE, 451–473.

Cullen, A. C. and Frey, H. C.: 1999, *Probabilistic Techniques in Exposure Assessment – A Handbook for Dealing with Variability and Uncertainty in Models and Inputs*, Plenum Press, New York.

Dyck, S. and Peschke, G.: 1995, *Grundlagen der Hydrologie*, Verlag für Bauwesen, Berlin.

Grothmann, T. and Reusswig, F.: 2006, People at Risk of Flooding: Why Some Residents Take Precautionary Action While Others do not. *Nat. Hazards* **38**, 101–120.

Holz, K.-P., Hildebrandt, G., and Weber, L.: 2006, Concept for a Web-based Information System for Flood Management. *Nat. Hazards* **38**, 121–140.

Kamrath, P., Disse, M., Hammer, M., and Köngeter, J.: 2006, Assessment of Discharge through a Dike Breach and Simulation of Flood Wave Propagation. *Nat. Hazards* **38**, 63–78.

Kortenhaus, A. and Oumeraci, H.: 2002, Probabilistische Bemessungsmethoden für Seedeiche (ProDeich). Bericht No. 877, Leichtweiss-Institut für Wasserwirtschaft, TU Braunschweig, (http://www.tu-bs.de/institute/lwi/hyku/german/Berichte/LWI_877.pdf).

Maidment, D. R.: 1992, *Handbook of Hydrology*, McGraw-Hill, New York.

Menzel, L., Thieken, A., Schwandt, D., and Bürger, G.: 2006, Impact of Climate Change on the Regional Hydrology – Scenario-Based Modelling Studies in the German Rhine Catchment. *Nat. Hazards* **38**, 45–61.

Plate, E. J.: 1992, Stochastic design in hydraulics: concepts for a broader application. in: *Proc. 6th IAHR Intern. Symp. on Stochastic Hydraulics*, Taipei, 1–15.

Singh, V. P.: 1996, *Dam Breach Modeling Technology*, Kluwer Academic Publishers, Dordrecht.

Stewart, M. G. and Melchers, R. E.: 1997, *Probabilistic Risk Assessment of Engineering Systems*, Chapman and Hall, London.

USACE (U.S. Army Corps of Engineers): 1999, Risk-based analysis in geotechnical engineering for support of planning studies. Engineer Technical Letter (ETL) 1110–2-556. Washington DC.

Vrijling, J. K.: 2000, Probabilistic Design – Lecture Notes. IHE Delft.

Vrijling, J.K.: 2001, Probabilistic design of water defense systems in The Netherlands, *Reliab. Eng. Syst. Safety* **74**, 337–344.

Wood, E. F. and Rodriguez-Iturbe, I.: 1975, A Baysian approach to analyzing uncertainty among flood frequency models, *Water Resour. Res.* **11**(6), 839–843.